2-(N,N-Dimethylamino)ethylselenolates of cadmium(II): Syntheses, structure of [Cd3(OAc)2(SeCH2CH2NMe2)4] and their use as single source precursors for the preparation of CdSe nanop...

ARTICLE *in* POLYHEDRON · AUGUST 2006

Impact Factor: 2.01 · DOI: 10.1016/j.poly.2006.02.011

Available online at www.sciencedirect.com
SCIENCE DIRECT
Polyhedron 25 (2006) 2383–2391
POLYHEDRON
www.elsevier.com/locate/poly

2-(*N*,*N*-Dimethylamino)ethylselenolates of cadmium(II): Syntheses, structure of $[Cd_3(OAc)_2(SeCH_2CH_2NMe_2)_4]$ and their use as single source precursors for the preparation of CdSe nanoparticles

G. Kedarnath [a], Sandip Dey [a], Vimal K. Jain [a,*], Gautam K. Dey [b], Babu Varghese [c]

[a] *Chemistry Division, Bhabha Atomic Research Centre, Trombay, Mumbai, Maharasthra 400085, India*
[b] *Materials Science Division, Bhabha Atomic Research Centre, Mumbai 400085, India*
[c] *RSIC, Indian Institute of Technology, Chennai 600036, India*

Received 8 November 2005; accepted 2 February 2006
Available online 9 March 2006

Abstract

The reaction of $Cd(OAc)_2 \cdot 2H_2O$ with $NaSeCH_2CH_2NMe_2$ gave a homoleptic cadmium selenolate, $[Cd(SeCH_2CH_2NMe_2)_2]$. The latter complex, on treatment with $Cd(OAc)_2 \cdot 2H_2O$, afforded $[Cd_3(OAc)_2(SeCH_2CH_2NMe_2)_4]$, which was structurally characterized by single-crystal X-ray diffraction analysis. Pyrolysis of $[Cd(SeCH_2CH_2NMe_2)_2]$ either in a mixture of hot hexadecylamine (HDA) and tri-*n*-octylphosphine oxide (TOPO) or in a furnace (180 and 200 °C) gave CdSe nanoparticles with average sizes varying between 3 and 21 nm. Both cubic and hexagonal phases of CdSe nanoparticles have been isolated under different experimental conditions. The CdSe nanoparticles were characterized by UV–Vis, photoluminescence, X-ray diffraction and electron microscopy. Time resolved luminescence measurements showed three different decay times for both band edge and trap state emissions.

Keywords: Cadmium selenolate; CdSe; Nanoparticles; Crystal structure; TEM

1. Introduction

Semiconductor nanoparticles [1,2], in particular II–VI, have been a subject area of considerable current research due to their promising applications in areas like catalysis [3], photovoltaics [4], materials for tunable LEDs [2,5] and biological imaging agents [6]. Among the II–VI nanoparticles, CdS and CdSe have been extensively studied owing to their tunable bandgap, making them potential candidates for bio-marking [7]. Shape selective synthesis of CdSe nano-rods [8–11], nano-wires [12], nano-tubes [13], nano-saw [14] and nano-arrows [15], have been reported, although simultaneous control of the shape, size and distribution of nanoparticles has been a challenging task. These materials have been synthesized by various techniques [16–23], which include pyrolysis of organometallic compounds [8,17–20], single source precursors [21] and solvothermal reactions [22]. Simple organochalcogenolates of zinc and cadmium are in general polymeric in nature and hence have limited utility as molecular precursors for II–VI materials [24]. We have recently reported the chemistry of internally functionalized chalcogenolate ligands, viz. *N*,*N*-dimethylaminoethylchalcogenolates which assist in suppressing polymerization [25,26]. For instance, the zinc complex $[Zn(SeCH_2CH_2NMe_2)_2]$, isolated as a discrete monomer, on pyrolysis afforded ZnSe [27]. This has prompted us to prepare the analogous cadmium complex and assess its suitability as a molecular precursor for CdSe nanoparticles. Results of this work are reported herein.

* Corresponding author. Tel.: +91 22 2559 5095; fax: +91 22 2550 5150.
E-mail addresses: jainvk@apsara.barc.ernet.in (V.K. Jain), varghese@iitm.ac.in (B. Varghese).

0277-5387/$ - see front matter © 2006 Elsevier Ltd. All rights reserved.
doi:10.1016/j.poly.2006.02.011

2. Experimental

2.1. Materials and methods

Cadmium acetate, mercury acetate, tmeda (*N*,*N*,*N*′,*N*′-tetramethylethylenediamine), tri-*n*-octylphosphineoxide (TOPO) and hexadecylamine (HDA) were obtained from commercial sources and were used without further purification. $HgCl_2 \cdot$ tmeda was prepared by refluxing $HgCl_2$ and excess tmeda in dichloromethane under an inert atmosphere for 2 h. Bis(2-dimethylaminoethyl)diselenide was prepared according to the literature method [25]. Solvents were dried and distilled before use under a nitrogen atmosphere. HPLC grade toluene was used in all experiments involved with a capping agent and pyridine was used in pyrolysis experiments for optical studies. Melting points were determined in capillary tubes and are uncorrected. Elemental analyses were carried out by the Analytical Chemistry Division of B.A.R.C. ^{1}H and $^{13}C\{^1H\}$ NMR spectra were recorded on a Bruker DPX-300 NMR spectrometer operating at 300 and 75.47 MHz, respectively. Chemical shifts are relative to the internal chloroform peak at δ 7.26 for ^{1}H and δ 77.0 for $^{13}C\{^1H\}$. UV–Vis absorption spectra were recorded on a Chemito Spectrascan UV 2600 double beam UV–Vis spectrophotometer. Fluorescence spectra were recorded using a Hitachi F-4010 spectrofluorometer. Time-resolved fluorescence measurements were carried out using a diode laser based time-correlated-single-photon-counting (TCSPC) spectrometer. In the present investigation, a 408 nm diode laser (1 MHz) was used as the excitation source and a TBX4 detection module coupled with a special Hamamatsu PMT was used for fluorescence detection. The instrument response function was ~230 ps at the FWHM. IR spectra were recorded on a Bomem MB-102 FT-IR spectrometer. Thermogravimetric analyses (TGA) were carried out on a Mettler TA–3000 instrument, which was calibrated with $CaC_2O_4 \cdot H_2O$. TG curve was recorded at a heating rate of 10 °C min^{-1} under a flow of nitrogen. X-ray powder diffraction data were collected on a Philips X-ray diffractometer (Model PW 1729) using Cu Kα radiation. A JEOL-2000FX transmission electron microscope operating at accelerating voltages up to 200 kV was used for TEM studies. The samples for TEM and SAED were prepared by placing a drop of a dilute solution of nanoparticles in acetone or pyridine on a carbon coated copper grid. EDAX was performed using a JEOL JSM-T330A instrument.

2.2. Synthesis of complexes

2.2.1. $[Cd(SeCH_2CH_2NMe_2)_2]$

A dichloromethane suspension (20 cm^3) of $Cd(OAc)_2 \cdot 2H_2O$ (664 mg, 2.49 mmol) was added to a freshly prepared methanolic solution of $NaSeCH_2CH_2NMe_2$ [prepared from $(Me_2NCH_2CH_2Se)_2$ (757 mg, 2.51 mmol) and $NaBH_4$ (193 mg, 5.10 mmol)] with continuous stirring at room temperature. After 3 h the colorless solution was dried in vacuo and the oily residue was washed with hexane and dried again in vacuo. The residue was extracted with CH_2Cl_2 (3×10 cm^3), filtered to remove NaOAc and the filtrate was evaporated under reduced pressure to give a white solid, which was recrystallized from dichloromethane-ethylacetate mixture. Yield: 702 mg (68%). mp 93–95 °C. *Anal.* Calc. for $C_8H_{20}N_2CdSe_2$: C, 23.2; H, 4.8; N, 6.8. Found: C, 23.0; H, 4.9; N, 6.6%. ^{1}H NMR (in $CDCl_3$) δ: 2.28 (s, NMe_2); 2.56 (br, $SeCH_2$); 2.74 (br, NCH_2). $^{13}C\{^1H\}$ NMR (in $CDCl_3$) δ: 15.5 (s, $SeCH_2$); 45.8 (s, NMe_2); 62.9 (s, NCH_2). The NMR spectra (^{1}H) in some samples showed additional peaks of low intensity (<5%) which may be attributed to $[Cd_3(OAc)_2(SeCH_2CH_2NMe_2)_4]$. The microanalysis of the latter (Calc. for $C_{20}H_{46}Cd_3N_4O_4Se_4$: C, 22.6; H, 4.3; N, 5.3%) is not significantly different from the bis derivative.

2.2.2. $[Cd_3(OAc)_2(SeCH_2CH_2NMe_2)_4]$

To a dichloromethane solution (5 cm^3) of $[Cd(SeCH_2CH_2NMe_2)_2]$ (187 mg, 0.45 mmol), a methanolic solution (5 cm^3) of $Cd(OAc)_2 \cdot 2H_2O$ (59 mg, 0.22 mmol) was added and the whole was heated at 40 °C with stirring for 2 h. The solvents were evaporated under vacuum and the residue was extracted with dichloromethane (5 cm$^3 \times 4$) and filtered through a fine filter. The filtrate was concentrated under vacuum to give a colorless powder (230 mg, 96%), mp 170 °C (dec. turns red). ν_{max}/cm^{-1} 1560 (C=O). ^{1}H NMR (in $CDCl_3$) δ: 2.05 (s, O_2CMe); 2.33 (s, NMe_2); 2.63 (br, $SeCH_2$); 2.82 (br, NCH_2). $^{13}C\{^1H\}$ NMR (in $CDCl_3$) δ: 16.4 (s, $SeCH_2$, ^1J(Se–C) = 57 Hz); 21.6 (s, O_2CMe); 45.5 (s, NMe_2); 62.0 (s, NCH_2); 179.4 (s, C=O).

2.2.3. Attempted preparation of $[Hg(SeCH_2CH_2NMe_2)_2]$

A dichloromethane solution (20 cm^3) of $HgCl_2 \cdot$ tmeda (201 mg, 0.51 mmol) was added to a freshly prepared methanolic solution of $NaSeCH_2CH_2NMe_2$ [prepared from $(Me_2NCH_2CH_2Se)_2$ (159 mg, 0.53 mmol) and $NaBH_4$ (44 mg, 1.16 mmol)] with continuous stirring at room temperature. After 3 h, a black precipitate settled down. The supernatant was decanted and the black precipitate was washed with hexane, acetone in sequence and then with water, acetone and dried in vacuo. Found: C, 1.8; H, 0.2; N, <0.2%. XRD pattern of this black powder was well in agreement with the pattern for cubic HgSe (JCPDS File No.73-1668). Similar results were obtained when $Hg(OAc)_2$ was used in place of $[HgCl_2 \cdot$ tmeda].

2.3. Synthesis of CdSe nanoparticles

2.3.1. Pyrolysis of $[Cd(SeCH_2CH_2NMe_2)_2]$ in HDA–TOPO mixture

In a three necked flask fitted with a thermometer, a continuously stirred mixture of HDA (2.39 g) and TOPO (185 mg) was degassed at 120 °C under argon atmosphere for 1 h. The temperature was slowly raised to 187 °C and stabilised at this temperature. To this, a solution of $[Cd(SeCH_2CH_2NMe_2)_2]$ (140 mg, 0.34 mmol) in a mixture

of dichloromethane (2 cm^3), toluene (2 cm^3) and TOPO (200 mg) was injected rapidly. The temperature dropped to 160 °C and was slowly raised to and maintained at 185 °C. Fractions were collected at 4 min (***fraction 1***) and 6 min (***fraction 2***) in vials containing methanol (5 cm^3). The hot solution at the end of 30 min (***fraction 3***) was cooled down to 70 °C and methanol was added to precipitate red nanoparticles. The red floculate was given a thorough washing with methanol followed by centrifuging and drying under vacuum.

Under similar conditions, a larger quantity of $[Cd(SeCH_2CH_2NMe_2)_2]$ (414 mg, 1.00 mmol) was pyrolysed in a mixture of HDA (7.09 g) and TOPO (1.00 g) and the reaction was quenched after 20 min (***fraction 4***) by adding methanol.

2.3.2. Pyrolysis of $[Cd(SeCH_2CH_2NMe_2)_2]$ in a furnace

Pyrolysis of $[Cd(SeCH_2CH_2NMe_2)_2]$ was carried out in a furnace under different conditions. In each experiment a weighed quantity (~80 mg) of the complex was dispersed in a small quartz boat by using dichloromethane and was subjected to pyrolysis. In one experiment the boat containing the complex was rapidly introduced into a preheated (180 °C) furnace and was kept at this temperature for 1 h under flowing nitrogen whereupon a yellowish-orange coat of CdSe (***fraction 5***: Found: C, 6.3; H, 1.8; N, 2.8%) was formed. In other experiments the furnace temperature was raised from room temperature to 200 °C in 5 min and the samples were heated at this temperature for 1 h either under flowing N_2 (***fraction 6***: Found: C, 6.9; H, 1.2; N, 1.6%) or under vacuum (***fraction 7***: Found: C, 5.6; H, 1.0; N, 1.6%), leading to the formation of a dark red CdSe coat. For optical measurements, small quantities of ***fractions 5–6*** were immediately dissolved in pyridine.

Table 1
Crystallographic and refinement data for $[Cd_3(OAc)_2(SeCH_2CH_2NMe_2)_4]$

Chemical formula	$C_{20}H_{46}Cd_3N_4O_4Se_4$
Formula weight	1059.65
Crystal size (mm^3)	$0.2 \times 0.2 \times 0.1$
Wavelength (Å)	0.71069
Crystal system	monoclinic
Space group	C_2/c
Unit cell dimensions	
a (Å)	24.700 (5)
b (Å)	13.309 (3)
c (Å)	11.575 (3)
β (°)	115.38 (4)
V ($Å^3$)	3437.8 (14)
D_{calc} ($g\,cm^{-1}$)	2.047
Z	4
μ (mm^{-1})	6.012
$F(000)$	2024
θ Range for data collection (°)	2.33–25.00
Limiting indices	$0 \leqslant h \leqslant 29$; $0 \leqslant k \leqslant 15$; $-13 \leqslant l \leqslant 12$
Reflections collected/unique (R_{int})	3245/3034 (0.0559)
Absorption correction	ψ scan
Data/restraints/parameters	3034/128/193
Final R_1 [$I > 2\sigma(I)$], ωR_2	0.0579, 0.1586
R_1, ωR_2 (all data)	0.1277, 0.1895
Largest difference in peak and hole (e $Å^{-3}$)	1.002 and −0.774

2.4. Crystallography

X-ray data of a colorless crystal of $[Cd_3(OAc)_2(SeCH_2CH_2NMe_2)_4]$ were collected at room temperature on an Enraf-Nonius CAD-4 diffractometer using graphite monochromated Mo Kα radiation ($\lambda = 0.71069$ Å) and employing the ω–2θ scan technique. The unit cell parameters (Table 1) were determined from 25 reflections measured by a random search routine. The intensity data were corrected for Lorentz, polarization and absorption effects (ψ scans). The structure was solved by direct methods using the SIR-92 program. The structure was completed by successive Fourier synthesis and refined using the SHELXL-97 program. The non-hydrogen atoms were refined with anisotropic thermal parameters. Hydrogen atoms could not be located reliably through difference Fourier maps due to disorder of the carbon atoms and hence were ignored.

3. Results and discussion

3.1. Synthesis and spectroscopy

Reaction of $Cd(OAc)_2 \cdot 2H_2O$ with $NaSeCH_2CH_2NMe_2$, prepared by the reduction of $(Me_2NCH_2CH_2Se)_2$ with $NaBH_4$ in methanol, gave a colorless homoleptic selenolate complex $[Cd(SeCH_2CH_2NMe_2)_2]$ (Eq. (1)). The freshly prepared complex is soluble in CH_2Cl_2, $CHCl_3$, benzene, toluene and methanol, but solubility decreases with aging, finally leading to a poorly soluble product. The NCH_2 and $SeCH_2$ proton resonances in the ^1H NMR spectrum appeared as broadened triplets which were shielded from the corresponding resonances for $(Me_2NCH_2CH_2Se)_2$. Several attempts to recrystallize the product from a mixture of solvents (CH_2Cl_2–hexane, CH_2Cl_2–MeCOOEt) gave either a colorless powder or flakes from which in some cases a few cubic crystals were separated which were identified by X-ray crystallography as a trinuclear cadmium complex, $[Cd_3(OAc)_2(SeCH_2CH_2NMe_2)_4]$. The latter complex, however, can readily be prepared by a redistribution reaction between $Cd(OAc)_2 \cdot 2H_2O$ and the bis complex, $[Cd(SeCH_2CH_2NMe_2)_2]$. Attempts to prepare the mercury complex, $[Hg(SeCH_2CH_2NMe_2)_2]$ using reaction route 1 led to excessive decomposition with the formation of cubic HgSe at room temperature.

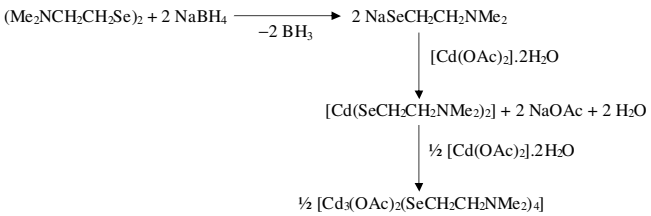

(1)

3.2. Crystal structure of $[Cd_3(OAc)_2(SeCH_2CH_2NMe_2)_4]$

The molecular structure of $[Cd_3(OAc)_2(SeCH_2CH_2NMe_2)_4]$, established unambiguously by X-ray diffraction analysis, is shown in Fig. 1 and selected interatomic parameters are listed in Table 2. The molecule has a twofold rotation axis passing through the central cadmium atom and hence half the molecule forms the crystallographic asymmetric unit. The $Me_2NCH_2CH_2Se$ fragments in the molecule are disordered and act in a chelating bridging fashion. The two terminal cadmium atoms adopt a skew trapezoidal planar geometry in which the basal plane is defined by two O and two Se atoms. The two remaining positions are occupied by the N atoms which are almost linear (∠N(1)–Cd(1)–N(2) 178.2 (3)°). The acetate ligand is asymmetrically chelated with two slightly different Cd–O distances, whereas the two C–O distances are essentially similar. The two Cd–Se distances differ marginally.

The coordination around the central cadmium is defined by four selenium bridges and adopts a pyrimidalized configuration with various angles varying between the ideal values of tetrahedral (109°) and square plane (90°). The two Cd–Se bonds are shorter than the other two. All the Cd–Se [28,29], Cd–N [28,30] and Cd–O [31] distances are well in agreement with values reported in other complexes.

Table 2
Selected bond lengths (Å) and angles (°) for $[Cd_3(OAc)_2(SeCH_2CH_2NMe_2)_4]$

Cd(1)–O(1)	2.311 (9)	Cd(2)–Se(1)	2.538 (3)
Cd(1)–O(2)	2.395 (9)	Cd(2)–Se(1′)	2.729 (3)
Cd(1)–Se(1)	2.724 (3)	Cd(2)–Se(2)	2.726 (3)
Cd(1)–Se(1′)	2.732 (3)	Cd(2)–Se(2′)	2.618 (3)
Cd(1)–Se(2)	2.800 (3)	Se(1)–C(6)	1.96 (2)
Cd(1)–Se(2′)	2.652 (2)	Se(1′)–C(10′)	2.03 (3)
Cd(1)–N(1)	2.413 (9)	Se(2)–C(10)	1.91 (3)
Cd(1)–N(2)	2.437 (12)	Se(2′)–C(6′)	2.06 (3)
O(1)–Cd(1)–O(2)	54.4 (3)	O(1)–Cd(1)–Se(2)	151.5 (3)
O(1)–Cd(1)–N(1)	93.5 (4)	O(2)–Cd(1)–Se(2)	101.5 (2)
O(2)–Cd(1)–N(1)	90.9 (3)	N(1)–Cd(1)–Se(2)	102.7 (2)
O(1)–Cd(1)–N(2)	88.0 (4)	N(2)–Cd(1)–Se(2)	76.3 (3)
O(2)–Cd(1)–N(2)	90.7 (4)	Se(1)–Cd(1)–Se(2)	96.14 (9)
N(1)–Cd(1)–N(2)	178.2 (3)	Se(1)–Cd(2)–Se(2)	102.61 (9)
O(1)–Cd(1)–Se(1)	109.3 (3)	Se(1′)–Cd(2)–Se(2′)	99.51 (8)
O(2)–Cd(1)–Se(1)	162.1 (2)	Cd(1)–Se(1)–Cd(2)	82.74 (9)
N(1)–Cd(1)–Se(1)	82.1 (2)	Cd(1)–Se(1′)–Cd(2)	79.20 (7)
N(2)–Cd(1)–Se(1)	96.4 (3)	Cd(1)–Se(2)–Cd(2)	78.07 (7)

3.3. Thermal studies

The TG curve (Fig. 2) of $[Cd(SeCH_2CH_2NMe_2)_2]$ showed that the complex decomposed in a single step at 155 °C to CdSe as inferred from the weight loss (Found: weight loss 52.6%; calcd. weight loss 53.8%).

Pyrolysis of $[Cd(SeCH_2CH_2NMe_2)_2]$ was carried out under different conditions, either in HDA/TOPO mixture or in a furnace. Pyrolysis of $[Cd(SeCH_2CH_2NMe_2)_2]$ in a furnace gave either cubic (***fractions 5*** and ***6***) or hexagonal (***fraction 7***) CdSe nanoparticles (from XRD, see later) which were formed under a flowing inert gas or vacuum, respectively. The microanalyses data of ***fractions 5–7*** suggest that the CdSe may be capped by the amine residues evolved on pyrolysis of the complex.

Pyrolysis of $[Cd(SeCH_2CH_2NMe_2)_2]$ in a HDA/TOPO mixture gave HDA capped CdSe nanoparticles. The IR

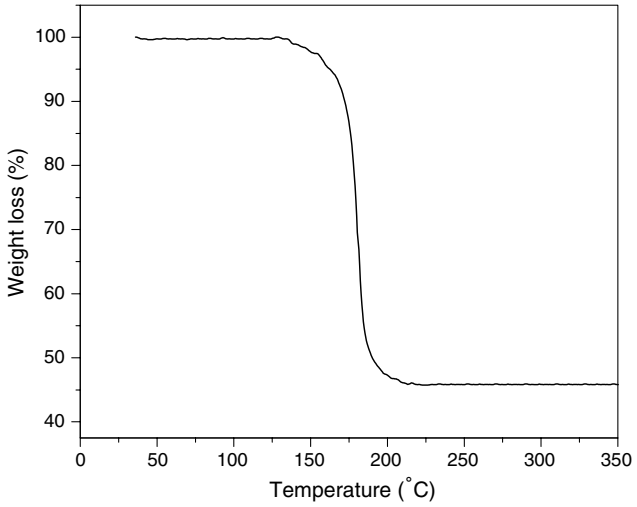

Fig. 2. TG curve of $[Cd(SeCH_2CH_2NMe_2)_2]$.

spectra of ***fractions 1–4*** (Fig. 3) displayed a shift of ν(N–H) to lower wavenumbers compared to that of free HDA (for free HDA ν(N–H) = 3333 cm^{-1}), indicating coordination of HDA. The $^{31}P\{^1H\}$ NMR chemical shifts for

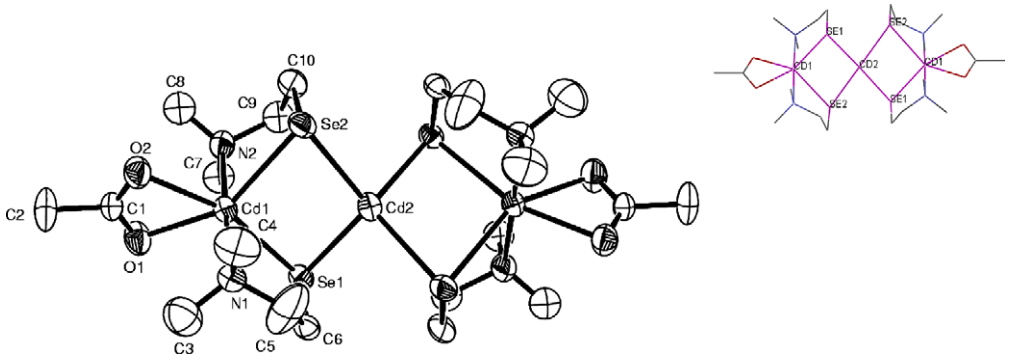

Fig. 1. ORTEP of $[Cd_3(OAc)_2(SeCH_2CH_2NMe_2)_4]$ with the atomic numbering scheme. Inset shows skeletal atoms.

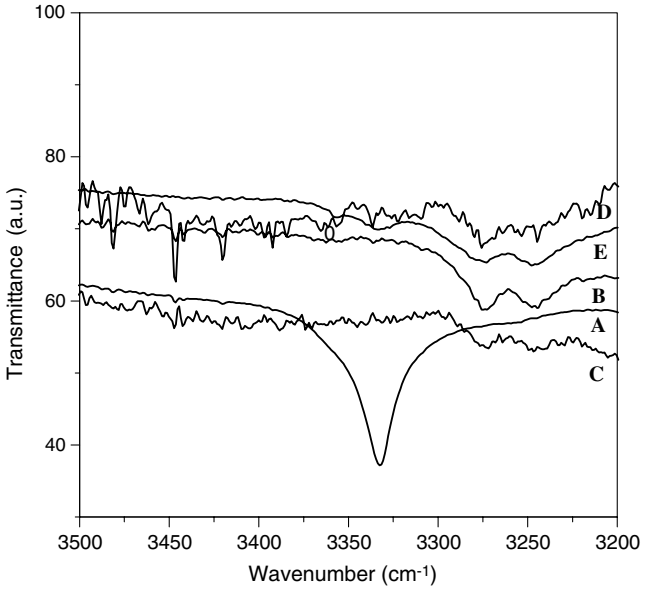

Fig. 3. IR spectra of **A**: free HAD, **B**: ***fraction 1***, **C**: ***fraction 2***, **D**: ***fraction 3*** and **E**: ***fraction 4***.

fraction 4 (δ 44.0 ppm) and free TOPO (δ 43.5 ppm) are comparable suggesting the absence of TOPO capping of CdSe nanoparticles.

3.4. Powder X-ray diffraction

XRD patterns (Fig. 4) of CdSe prepared by pyrolysis of $[Cd(SeCH_2CH_2NMe_2)_2]$ under different conditions showed broad peaks which are typical for particles in the nano regime. The particle sizes estimated from Scherrer's formula come out to be 12, 6, 4, 9 and 8.3 nm for ***fractions 3***, ***4***, ***5***, ***6*** and *7*, respectively. The pattern can be assigned to the cubic phase of CdSe in the case of ***fractions 5*** and ***6*** and the hexagonal phase of CdSe in the case of ***fraction 7*** (Table 3). In the case of ***fraction 7***, we have used X-ray peak fitting software to confirm whether the first peak is a single peak or the overlap of three peaks and it is fitted into three peaks, which coincides with the hexagonal phase of CdSe. Assignment of the hexagonal phase of CdSe to ***fraction 7*** is further confirmed by its SAED pattern.

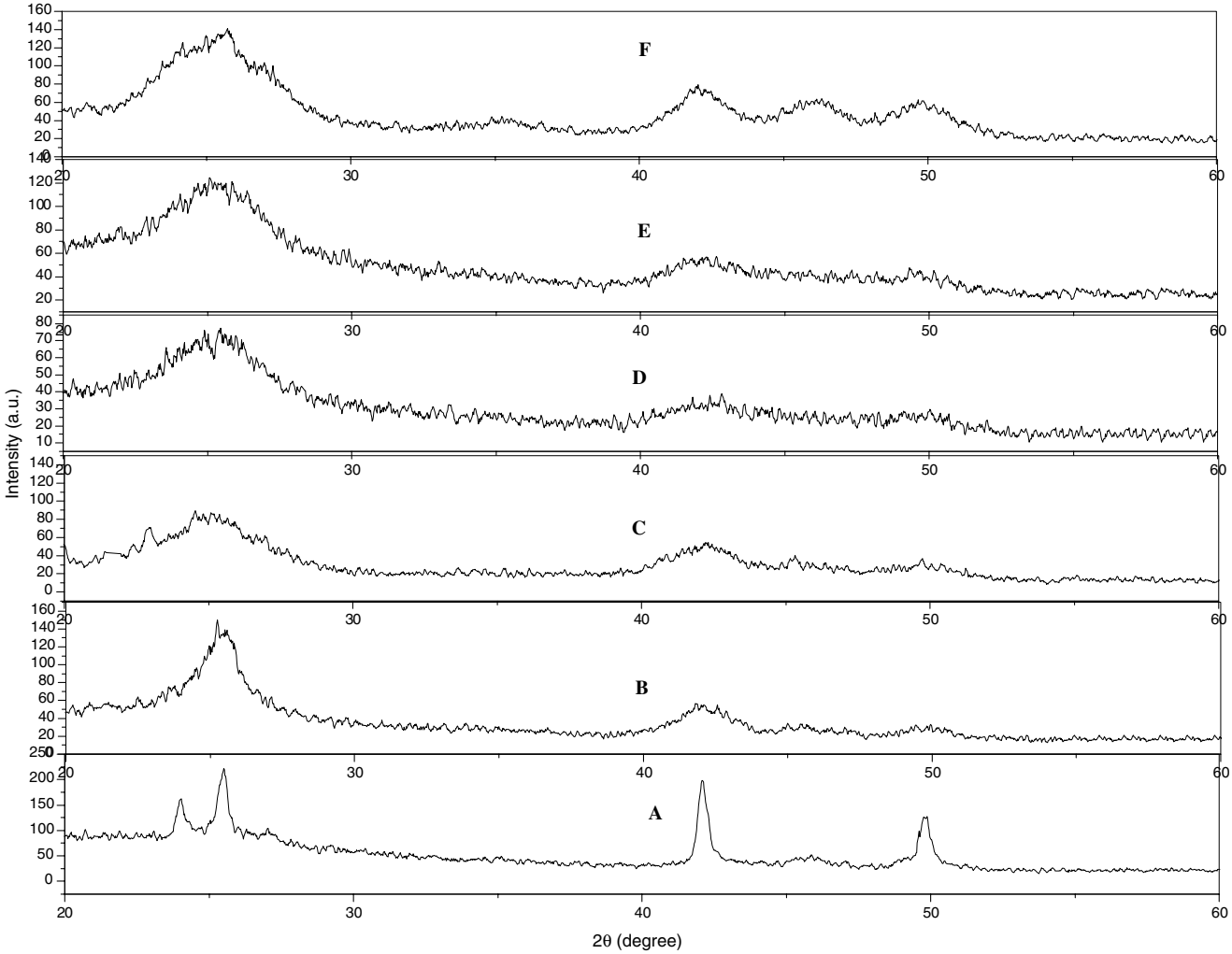

Fig. 4. XRD pattern of **A**: bulk CdSe obtained at 400 °C, **B**: ***fraction 3***, **C**: ***fraction 4***, **D**: ***fraction 5***, **E**: ***fraction 6*** and **F**: ***fraction 7***.

Table 3
XRD data of CdSe nanoparticles prepared by different routes and the particle sizes of different fractions

Fraction	XRD data				Size calculated from Brus expression (nm)	Size calculated from Scherrer's formula (nm)	Size obtained from TEM (nm)
	d (Å)			Lattice parameter (Å)			
1					5		
2					6.4		
3	3.49	2.15	1.83	6.046	12.2	12	
4	3.55	2.16	1.83	6.149	7.9	6	7.5
5	3.47	2.14	1.83	6.011	4.8	4	
6	3.54	2.15	1.83	6.131	6.7	9	
7	3.66	2.14	3.27	4.274, 6.958	6.5	8.3	21[c]
CdSe (cubic)[a]	3.51	2.15	1.83	6.077			
CdSe (hexagonal)[b]	3.72	2.15	3.29	4.299, 7.010			

[a] JCPDS File No. 80-0021 (International Centre for Diffraction data – 1998).
[b] JCPDS File No. 08-0459 (International Centre for Diffraction data – 1998).
[c] TEM of the sample was recorded after one month and therefore ripening might have taken place and hence a larger size compared to the one estimated from the XRD pattern.

3.5. Electron microscopy

The selected area electron diffraction (SAED) patterns of ***fractions 4*** and *7* (Fig. 5) revealed the formation of crystalline CdSe. Clear diffraction rings corresponding to the lattice planes (111), (220) and (311) in the SAED pattern of the ***fraction 4*** were attributed to cubic CdSe. The SAED pattern of ***fraction*** *7* has been interpreted in terms of the hexagonal phase of CdSe with diffraction rings corresponding to the lattice planes (100), (101), (102), (110), (103), (112), (202) and (203). The phases determined from the SAED and XRD patterns were in agreement with each other. The TEM images of ***fraction 4*** (Fig. 6) and ***fraction*** *7* (Fig. 7) shows the particles are spherical in shape. The average diameters of particles of ***fraction 4*** and ***fraction*** *7*, estimated from TEM images, are $7.5 \pm 4\%$ and $21 \pm 8\%$ nm, respectively. In the case of ***fraction 4***, the particle size obtained from the TEM image is closer to that of the particle size calculated from the XRD pattern using Scherrer's formula. EDX spectra of ***fractions 3***, ***4***, ***6*** and *7* exhibited peaks for Cd and Se, which were in 1:1 ratios.

3.6. Optical properties

CdSe nanoparticles, prepared by pyrolysis of $[Cd(SeCH_2CH_2NMe_2)_2]$ in a furnace, displayed absorption maxima at 423 (***fraction 5***), 538, 580 (***fraction 6***) and 455 nm (***fraction*** *7*) (Fig. 8). The excitation spectrum of ***fraction*** *7* at room temperature showed a broad exciton peak at 400 nm, whereas a broad maximum at 499 nm was observed in the emission spectrum (Fig. 8).

Absorption, excitation and emission spectra of HDA capped CdSe nanoparticles, prepared by pyrolysis of $[Cd(SeCH_2CH_2NMe_2)_2]$ in HDA/TOPO mixture are given in Figs. 9–11. Absorption spectra (Fig. 9) of HDA capped CdSe nanoparticles displayed a typical band edge absorption with an exciton band and the spectra are well in agreement with those reported earlier [17,19,32]. ***Fractions 1–4*** showed exciton maxima at 490, 549, 625 and 582 nm,

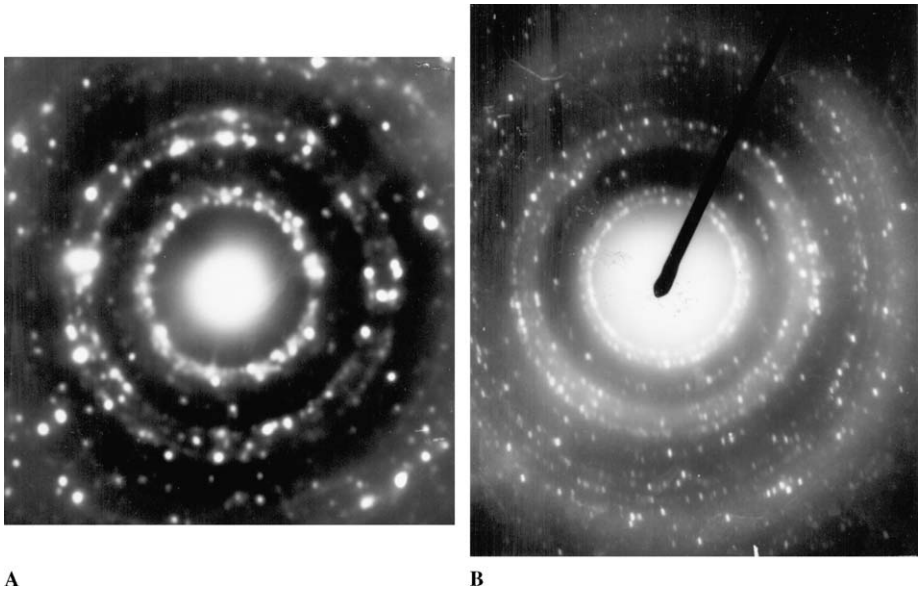

A B

Fig. 5. SAED pattern CdSe nanoparticles of **A**: ***fraction 4*** and **B**: ***fraction*** *7*.

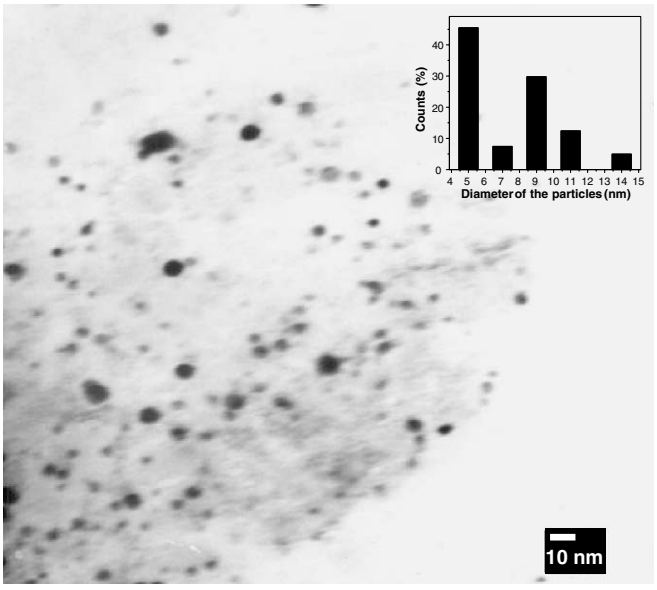

Fig. 6. TEM picture of capped CdSe nanoparticles of ***fraction 4***. Inset shows particle size distribution.

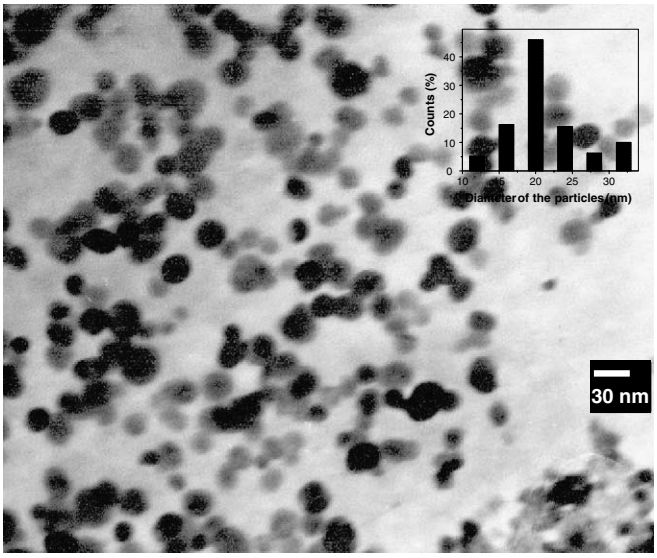

Fig. 7. TEM picture of CdSe nanoparticles of ***fraction 7***. Inset shows particle size distribution.

respectively, which are blue shifted with respect to bulk CdSe ($\lambda_{onset} = 713$ nm), confirming the quantum confinement effect of the particles. The absorption maximum of the fractions collected at different time intervals showed a red shift with increasing time, which is in accordance with earlier reports [33]. The excitation spectra (Fig. 10) for each fraction are found to have maxima at 494, 549 and 625 nm, respectively, at room temperature. These excitation maxima coincide well with the absorption band edges of the three ***fractions 1–3*** at 490, 547 and 625 nm, respectively. The emission spectra (Fig. 11) displayed two peaks each in ***fractions 1*** (518, 640 nm) and ***2*** (573 and 719 nm) corresponding to band edge and trap state emissions [34–36].

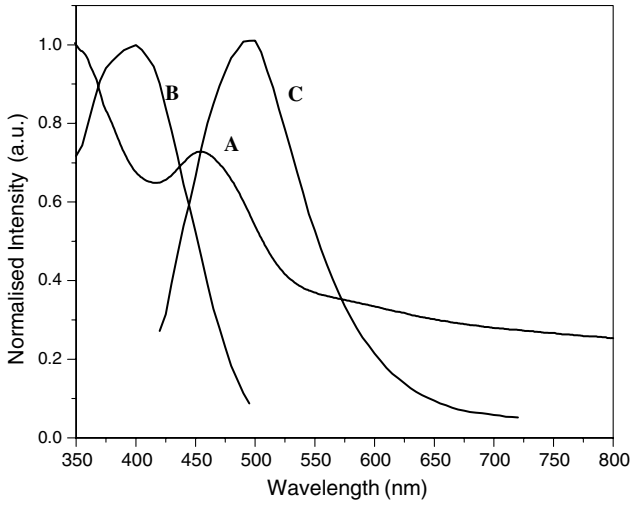

Fig. 8. **A**: Absorption spectrum, **B**: excitation spectrum and **C**: emission spectrum of CdSe nanoparticles of ***fraction 7***.

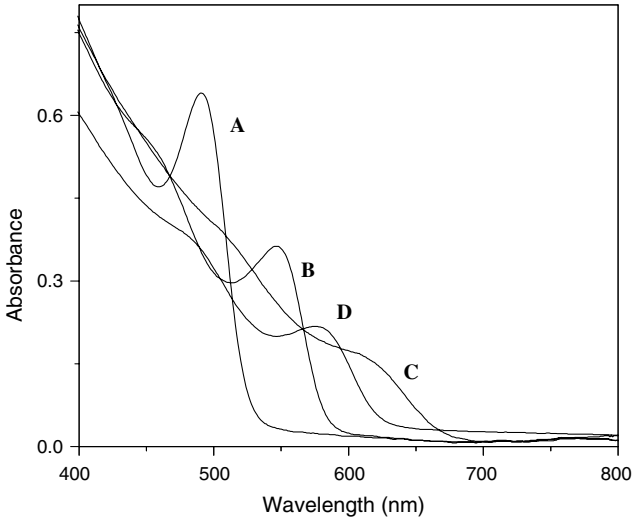

Fig. 9. Absorption spectra of HDA capped CdSe nanoparticles **A**: ***fraction 1***, **B**: ***fraction 2***, **C**: ***fraction 3*** and **D**: ***fraction 4***.

The spectra showed narrow band edge emission peaks in these fractions, implying that the particle size distribution is narrow as the width of the emission peaks depend on the size distribution of the particles [19]. The ***fractions 3*** and ***4***, however, showed only a broad and a narrow peak corresponding to band edge emissions at 637 and 605 nm, respectively, implying a slightly broad and narrow distribution of the particles in these fractions. The particle sizes estimated using Brus's expression [37] for the ***fractions 1–4*** are 5, 6.4, 12.2 and 7.9 nm, respectively, and compare well with the size estimated employing Scherrer's formula (Table 3).

To understand the charge carrier dynamics, we have carried out time-resolved luminescence measurements (Fig. 12) of ***fractions 1*** and ***3***. For all the samples, excitation was carried out at 408 nm. For ***fraction 1***, lifetimes for both the band edge and trap state components were taken while

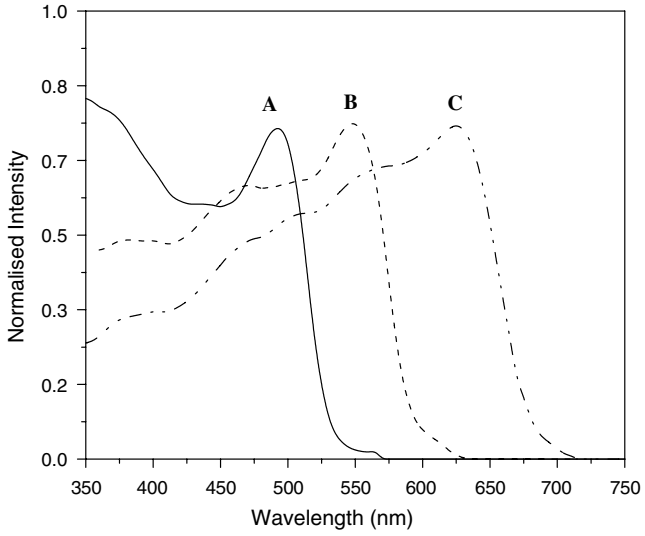

Fig. 10. Excitation spectra of HDA capped CdSe nanoparticles **A**: ***fraction 1***, **B**: ***fraction 2*** and **C**: ***fraction 3***.

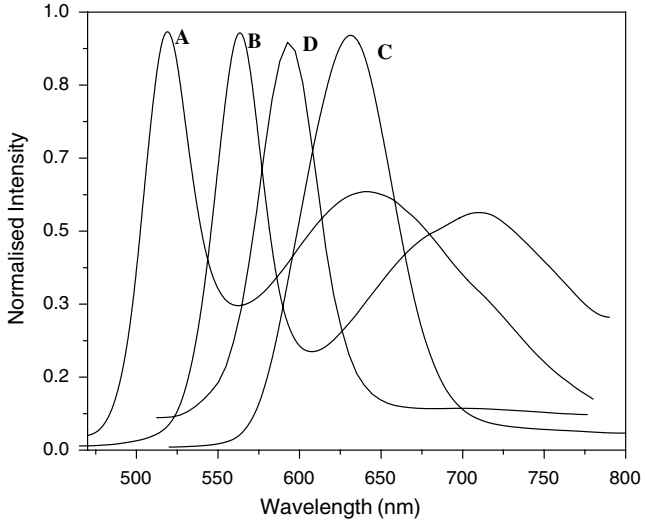

Fig. 11. Emission spectra of HDA capped CdSe nanoparticles **A**: ***fraction 1***, **B**: ***fraction 2***, **C**: ***fraction 3*** and **D**: ***fraction 4***.

for ***fraction 3***, the band edge component was studied. A multi-exponential function has been used to fit the data for a reasonable fit in all the cases. Three different decay times for each band edge [0.5 (68%), 8.3 (24%), 61.5 (8%) ns] and trap state components [1.8 (29%), 12.3 (36%), 73.7 (35%) ns] for ***fraction 1*** were observed. Similarly three decay times [2.9 (45%), 12.5 (46%) and 49.1 (9%) ns] for the band edge emission for ***fraction 3*** were identified. The multi-exponential character of the decay, even when photoluminescence shows well resolved lines, can be attributed to the overlap of various contributions arising from different particles [38]. The decay times of band edge and trap state emission of ***fraction 1*** shows that the former component is faster than the latter. The decay times of the band edge component of ***fraction 1*** is also faster than that of ***fraction 3***, showing size dependence of life times and is in agreement with the reported data [32].

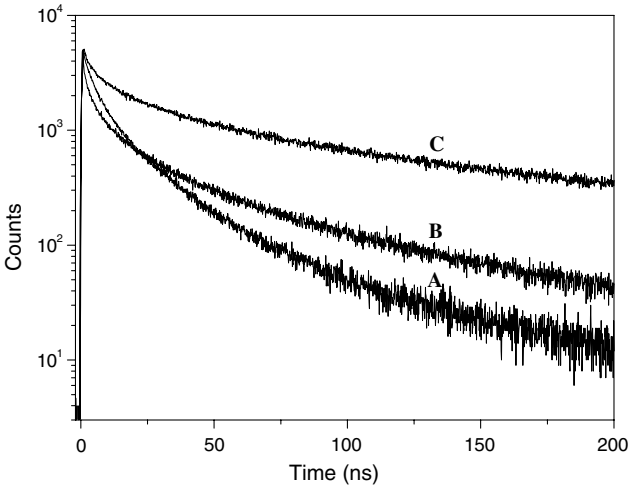

Fig. 12. Lifetime measurements of **A**: band edge component of ***fraction 3***, **B**: band edge component of ***fraction 1*** and **C**: trap state component of ***fraction 1***.

4. Conclusion

The single source precursor $[Cd(SeCH_2CH_2NMe_2)_2]$, prepared conveniently, has been employed for the synthesis of CdSe nanoparticles. The size and phase (cubic and hexagonal) of these particles is conveniently controlled by varying the pyrolysis conditions. Both absorption and emission bands of these nanoparticles showed size dependence and were blue shifted with decreasing particle size. The band edge and trap state showed three different decay times.

5. Supplementary materials

CCDC-277552 contains the supplementary crystallographic data for this paper. These data can be obtained free of charge at www.ccdc.cam.ac.uk/conts/retrieving.html or from the Cambridge Crystallographic Data Centre, 12 Union Road, Cambridge CB2 1EZ, UK [fax: (internat.) +44 1223 336 033; e-mail: deposit@ccdc.cam.ac.uk].

Acknowledgements

We thank Drs. T. Mukherjee and S.K. Kulshreshtha for encouragement of this work. We are also grateful to Dr. M. Sudarsanan, Head, Analytical Chemistry Division for providing microanalyses of the complexes and Dr. G. Ramakrishna for helpful discussions.

References

[1] T. Trindade, P. O'Brien, N.L. Pickett, Chem. Mater. 13 (2001) 3843.
[2] M. Nirmal, L. Brus, Acc. Chem. Res. 32 (1999) 407.
[3] T.S. Ahmadi, Z.L. Wang, T.C. Green, A. Henglein, M.A. Elsayed, Science 272 (1996) 1924.
[4] W. Huynch, X.G. Peng, A.P. Alivisatos, Adv. Mater. 11 (1999) 923.
[5] L.H. Qu, Z.A. Peng, X.G. Peng, Nano Lett. 1 (2001) 331.

[6] (a) W.C.W. Chan, S. Nie, Science 281 (1998) 2016;
(b) D.R. Larson, W.R. Zipfel, R.W. Williams, S.W. Clark, M.P. Bruchez, F.W. Wise, W.W. Webb, Science 300 (2003) 1434;
(c) M. Green, Angew. Chem., Int. Ed. 43 (2004) 4129.
[7] J.W. Jlot, H.J. Geuze, J. Cell. Biol. 90 (1981) 533.
[8] X.G. Peng, L. Manna, W.D. Yang, J. Wickham, E. Scher, A. Kadavanich, A.P. Alivisatos, Nature 404 (2000) 59.
[9] J.T. Hu, L.S. Li, W.D. Yang, L. Manna, L.W. Wang, A.P. Alivisatos, Science 292 (2001) 2060.
[10] L.S. Li, J. Hu, W. Yang, A.P. Alivisatos, Nano Lett. 1 (2001) 349.
[11] P.S. Nair, K.P. Fritz, G.D. Sckoles, Chem. Commun. (2004) 2084.
[12] M.S. Gudiksen, J. Wang, C.M. Lieber, J. Phys. Chem. B 106 (2002) 4036.
[13] X.C. Jiang, B. Mayers, T. Herricks, Y.N. Xia, Adv. Mater. 15 (2003) 1740.
[14] C. Ma, Y. Ding, D. Moore, X. Wang, Z.L. Wang, J. Am. Chem. Soc. 126 (2004) 708.
[15] L. Manna, E.C. Scher, A.P. Alivisatos, J. Am. Chem. Soc. 122 (2000) 12700.
[16] M. Green, P. O'Brien, Chem. Commun. (1999) 2235.
[17] C.B. Murray, D.J. Norris, M.G. Bawendi, J. Am. Chem. Soc. 115 (1993) 8706.
[18] M. Grätzel, Nature 338 (1989) 540.
[19] M.A. Malik, P. O'Brien, Adv. Mater. Opt. Electron. 3 (1994) 171.
[20] P. Reiss, J. Bleuse, A. Pron, Nano Lett. 2 (2002) 781.
[21] (a) D.J. Crouch, P. O'Brien, M.A. Malik, P.J. Skabara, S.P. Wright, Chem. Commun. (2003) 1454;
(b) M.A. Malik, N. Revaprasadu, P. O'Brien, Chem. Mater. 13 (2001) 913.
[22] UK Gautam, M. Rajamathi, F. Meldrum, P. Morgan, R. Seshadri, Chem. Commun. (2001) 629.
[23] M.L. Steigerwald, A.P. Alivisatos, J.M. Gibson, T.D. Harris, R. Kortan, A.J. Muller, A.M. Thayer, T.M. Duncan, D.C. Douglass, L.E. Brus, J. Am. Chem. Soc. 110 (1988) 3046.
[24] D.E. Fenton, in: J.A. McCleverty, T.J. Meyer (Eds.), Comprehensive Coordination Chemistry–II, vol. 6, Pergamon Press, Oxford, 2004 p. 1253.
[25] S. Dey, V.K. Jain, S. Chaudhury, A. Knoedler, F. Lissner, W. Kaim, J. Chem. Soc., Dalton Trans. (2001) 723.
[26] (a) S. Dey, V.K. Jain, A. Knoedler, W. Kaim, S. Zalis, Eur. J. Inorg. Chem. (2001) 2965;
(b) S. Dey, V.K. Jain, A. Knoedler, W. Kaim, S. Zalis, Inorg. Chem. 41 (2002) 2864;
(c) S. Dey, V.K. Jain, A. Knoedler, W. Kaim, Indian J. Chem. A 42 (2003) 2339.
[27] S. Dey, V.K. Jain, S. Chaudhury, A. Knoedler, W. Kaim, Polyhedron 22 (2003) 489.
[28] Y. Cheng, T.J. Emge, J.G. Brennan, Inorg. Chem. 33 (1994) 3711.
[29] M.T. Ng, P.A.W. Dean, J.J. Vittal, J. Chem. Soc., Dalton Trans. (2004) 2890.
[30] M.D. Nyman, M.J. Hampden Smith, E.N. Duesler, Inorg. Chem. 36 (1997) 2218.
[31] R.S. Honkonen, P.D. Ellis, J. Am. Chem. Soc. 106 (1984) 5488.
[32] D.M. Mittleman, R.W. Schoenlein, J.J. Shiang, V.L. Colvin, A.P. Alivisatos, C.W. Shank, Phys. Rev. B 49 (1994) 14435.
[33] (a) S.D. Bunge, K.M. Krueger, T.J. Boyle, M.A. Rodriguez, T.J. Headley, V.L. Colvin, J. Mater. Chem. 13 (2003) 1705;
(b) H. Nakamura, Y. Yamaguchi, M. Miyazaki, H. Maeda, M. Uehara, P. Mulvaney, Chem. Commun. (2002) 2844.
[34] (a) A. Hasselbarth, A. Eychmuller, H. Weller, Chem. Phys. Lett. 203 (1993) 271;
(b) M.G. Bawendi, P.J. Carroll, W.L. Wilson, L.E. Brus, J. Chem. Phys. 96 (1992) 946.
[35] (a) R. Jaeger-Waldau, N. Stuecheli, M. Braun, M. Luse Steiner, E. Bucher, R. Tenne, H. Flaisher, W. Kerfin, R. Braun, W. Koschel, J. Appl. Phys. 64 (1988) 2601;
(b) J.Y. Lin, D. Baum, Q. Zhu, A. Honig, H.X. Jiang, J. Lumin. 45 (1990) 251.
[36] M. Nirmal, C.B. Murray, M.G. Bawendi, Phys. Rev. B 50 (1994) 2293.
[37] J.Z. Zhang, J. Phys. Chem. B 104 (2000) 7239.
[38] P. Lefebvre, H. Mathieu, J. Allegre, T. Richard, A. Combettes-Roos, M. Pauthe, W. Granier, Semicond. Sci. Technol. 12 (1997) 958.